Journal of Agriculture and Food Research 27 (2026) 102724

Contents lists available at ScienceDirect

Journal of Agriculture and Food Research

journal homepage: www.sciencedirect.com/journal/journal-of-agriculture-and-food-research

# Physiological and phytochemical responses of broccoli sprouts to micro/nanoplastics, elevated $CO_2$ and heat stress under a predictive modeling framework

Marcelo Illanes [a,b], María Trinidad Toro [c], Felipe Noriega [a,b], Mauricio Schoebitz [d], Roberto Fustos-Toribio [e], Nelson Zapata [a], Diego A. Moreno [f,*], María Dolores López-Belchí [a,b,**]

[a] Departamento de Producción Vegetal, Facultad de Agronomía, Universidad de Concepción, 4030000, Concepción, Chile
[b] Laboratorio de Bioactivos e Ingredientes Vegetales (BIOINVE), Centro de Biotecnología, Universidad de Concepción, 4030000, Concepción, Chile
[c] School of Nutrition and Dietetics, Faculty of Medicine and Health Science, Universidad Mayor, Temuco, Chile
[d] Department of Soils and Natural Resources, Faculty of Agronomy, University of Concepcion, Victor Lamas 1290, Concepción, Chile
[e] Department of Mining Engineering, Universidad de Concepción, 4030000, Concepción, Chile
[f] Laboratorio de Fitoquímica y Alimentos Saludables (LabFAS). CSIC, CEBAS. Campus Universitario de Espinardo-25, 30100, Murcia, Spain

ARTICLE INFO

*Keywords:*
Food production
Emergent contaminants
Environmental stress
Glucosinolates
Plant secondary metabolites
Predictive modelling

ABSTRACT

Broccoli sprouts (*Brassica oleracea* L. var. *italica*) are valuable sources of bioactive phytochemicals with nutritional and functional relevance. Their metabolic responses are highly sensitive to environmental factors, yet the combined effects of climate-related and contaminant stressors remain poorly understood. This study evaluated the interactive influence of elevated $CO_2$ (1000 ppm), temperature (28 °C), and micro/nanoplastics (MNPs) on the physiological and phytochemical responses of broccoli sprouts.

Temperature was the main driver, enhancing total glucosinolates (10–71%) but decreasing biomass (1–13%), revealing a clear growth–defense trade-off. $CO_2$ enrichment exerted moderate, context-dependent effects, stimulating glucosinolates and anthocyanins synthesis at 20 °C but attenuating them under heat. MNPs acted as secondary modulators, slightly influencing phytohormone and phenolic profiles through indirect interactions. Multivariate and neural-network modeling ($R^2$ = 0.86–0.94) confirmed temperature as the dominant factor leading metabolic reprogramming toward sulfur- and phenylpropanoid-based defenses.

These results demonstrate that predictive modeling can effectively integrate multistress physiological responses, offering new insights into plant adaptability and the functional quality of edible sprouts under future climate and contaminant scenarios.

## 1. Introduction

Micro- and nanoplastics (MNPs) are emerging pollutants in agroecosystems with increasing evidence of entry into the food chain, raising both ecological and human health concerns [1]. Their small size, surface reactivity, and ubiquity in soils enable interactions with the rhizosphere, affecting nutrient dynamics, water relations, and microbial associations [2]. Recent studies indicate that plants are able to absorb microplastics and nanoplastics through root tissues, potentially altering developmental trajectories and compromising plant–microbe interactions, including the fungi's ability to enhance water and nutrient uptake [3,4].

Concurrently, global agriculture faces accelerating pressures from elevated atmospheric $CO_2$ and rising temperatures—conditions that reshape primary metabolism, hormonal signaling, and the balance between growth and defense pathways in crops [5,6]. Elevated $CO_2$ can stimulate carbon assimilation, modify biomass allocation, and alter the synthesis of secondary metabolites, while heat stress frequently disrupts

* Corresponding author.
** Corresponding author. Departamento de Producción Vegetal, Facultad de Agronomía, Universidad de Concepción, 4030000, Concepción, Chile.
*E-mail addresses:* marceloillanes@udec.cl (M. Illanes), maria.toror@umayor.cl (M.T. Toro), fnoriega@udec.cl (F. Noriega), mschoebitz@udec.cl (M. Schoebitz), robertofustos@udec.cl (R. Fustos-Toribio), nzapata@udec.cl (N. Zapata), dmoreno@cebas.csic.es (D.A. Moreno), mlopezb@udec.cl (M.D. López-Belchí).

https://doi.org/10.1016/j.jafr.2026.102724
Received 9 November 2025; Received in revised form 24 January 2026; Accepted 26 January 2026
Available online 7 February 2026

photosynthetic efficiency, accelerates growth cycles, and reduces yield stability [7]. Beyond their individual impacts, interactions among $CO_2$, temperature, and soil-borne contaminants represent a multidimensional challenge for sustainable crop production. However, how plants integrate emerging contaminants (e.g., micro/nanoplastics) and climate drivers (elevated $CO_2$ and temperature) into coherent metabolic responses remains largely unknown.

From a conceptual perspective, micro- and nanoplastics, elevated $CO_2$, and heat represent interconnected components of the global-change pressures that increasingly define agricultural systems. Each factor can independently reshape plant metabolic baselines, modifying carbon allocation, hormonal signaling, oxidative balance, and defensive chemistry, yet their combined effects are unlikely to be predictable from single-stressor studies. Most existing research has evaluated these drivers in isolation, limiting our understanding of how plants integrate simultaneous pollutant and climate-related cues. Addressing these knowledge gaps requires experimental frameworks capable of disentangling additive, synergistic, or antagonistic interactions among MNPs, $CO_2$, and temperature under controlled yet ecologically relevant conditions.

The Brassicaceae family, which includes economically important crops such as broccoli, kale, and mustard, is characterized by complex phytochemical profiles, particularly glucosinolates, phenolics, and antioxidant compounds, highly responsive to environmental cues [8,9]. Broccoli sprouts, in particular, display rapid developmental rates and a strong sensitivity to early stress signals, making them powerful biomarkers for studying pollutant–climate interactions. Their relevance is amplified by their growing incorporation into functional foods, nutraceuticals, and health-promoting diets due to their dense content of bioactive metabolites.

Moreover, recent analyses highlight that the food industry is undergoing substantial structural stress, driven by global disruptions that have exposed persistent weaknesses in safety, supply stability, and nutritional resilience [10]. These pressures have intensified the demand for resilient, health-promoting foods, particularly those with functional or bioactive properties, as consumers increasingly shift toward minimally processed, plant-based ingredients [11]. In parallel, technological and sustainability transitions are pushing the sector toward circular production models, reduced resource use, and greater valorization of plant-derived compounds [12]. Within this evolving scenario, understanding how emerging contaminants and climate-related stressors modulate the nutritional and functional profile of Brassica sprouts becomes directly aligned with the current needs and future direction of the food industry.

Despite growing evidence that MNPs can affect plant growth and that elevated $CO_2$ and heat strongly modulate Brassica metabolism, their combined and potentially non-additive effects on hormonal balance, oxidative responses, biomass allocation, and health-promoting metabolites in edible sprouts remain largely unresolved. In particular, it is unknown (i) whether MNPs act as primary or secondary modulators across contrasting $CO_2$–temperature regimes, (ii) how global-change drivers reshape growth–defense trade-offs at early developmental stages, and (iii) whether such multidimensional responses can be captured using predictive modeling frameworks relevant to food quality and risk assessment. Broccoli sprouts, given their phytochemical richness and stress sensitivity, offer an ideal system to address these questions. Therefore, this study integrates polyethylene microplastics and polystyrene nanoplastics with factorial $CO_2$–temperature conditions, combining physiological, hormonal, antioxidant, and phytochemical profiling under a predictive modeling framework. We hypothesize that MNPs act as context-dependent modulators of sprout physiology and functional quality under concurrent pollutant and climate-related stressors.

## 2. Material and methods

### 2.1. Experimental design

Broccoli sprouts (*Brassica oleracea* L. var. italica) were grown in glass trays filled with coconut fiber substrate. Seeds (cv. Waltham-29) were obtained from Semillera San Alfonso (Santiago, Chile). Three substrate treatments were established: coconut fiber without plastic (WP), coconut fiber supplemented with polyethylene (PE) microplastics, and coconut fiber supplemented with polystyrene (PS) nanoplastics. Six replicate trays were prepared per treatment ($n = 6$), each containing 1 kg of substrate moistened with 700 mL of Milli-Q water.

For plastic treatments, aqueous suspensions of PE MPs or PS NPs were applied during initial substrate wetting to reach a nominal concentration of 500 mg $kg^{-1}$, previously reported as phytotoxic and selected based on prior dose-screening experiments in broccoli [13]. Subsequent irrigations were carried out with distilled water only.

Seeds were surface-sterilized with sodium hypochlorite, soaked for 24 h, and 5 g were sown per tray (day 0). Trays were incubated in darkness for three days to promote germination and then transferred to controlled-environment chambers. Twelve environmental treatments were applied, combining two temperature regimes (20/18 °C and 28/22 °C day/night) and two $CO_2$ concentrations (500 or 1000 ppm) across the three substrate conditions. Plants were grown under a 16 h light/8 h dark photoperiod (350 μmol $m^{-2}$ $s^{-1}$ PAR) and irrigated every two days. After 12 days, sprouts were harvested, weighed, and immediately frozen at −80 °C for biochemical analyses. Physicochemical properties of the coconut fiber substrate are provided in the Supplementary Materials (Table S1).

### 2.2. Preparation of polyethylene (PE)-MP and polystyrene (PS)-NP suspensions

Two types of plastic derivatives were used in this study: NPs derived from PS and MPs derived from PE. PS NPs were obtained from clean polystyrene boxes. The material was degraded using acetone at a ratio of 200 mL of acetone per 1 kg of polystyrene. The resulting polystyrene-acetone solution was transferred to laminar flow chambers to allow partial evaporation of acetone. Subsequently, the mixture was placed in an oven at 40 °C for 7 days to ensure complete dehydration. The dry polystyrene material was then pulverized using a ball mill in 2-min cycles until a nanoscale powder was obtained. PE were produced from high-density polyethylene (HDPE) pellets acquired from Sigma-Aldrich (St. Louis, MO, USA). The pellets were artificially aged for three months under ultraviolet (UV) radiation to simulate the environmental degradation. After aging, the pellets were mechanically ground using a laboratory ball mill to obtain the MPs particles. Particle size was analyzed by Laser analyzer Mastersizer 3000 (Malvern Instruments, Malvern, UK) and a Zetasizer Advanced Ultrared Label (Malvern Panalytical Ltd., UK), with granulometric parameters obtained via Gradistat v8.0. In addition, Fourier-transform infrared spectroscopy (FTIR) images of particles were collected using an FTIR spectrometer and microscope system (Spotlight 400, PerkinElmer). Finally, particles were analyzed by scanning electron microscopy (SEM, Vega3 Easyprobe SBU, Tescan). Samples (whole and cross-sections) were mounted on stubs with double-sided adhesive tape, gold-coated, and examined at 15 kV and 20 mm working distance. Topographical images were acquired at magnifications from 830 × to 7370 × (resolving structures in the 50 nm–5 μm range) and from 49 × to 1350 × (20 μm–1000 μm), enabling characterization at both micro- and nanoscale levels (Fig. S1). Zeta potential measurements were conducted to assess the surface charge and colloidal stability of MNP suspensions under the experimental conditions used in this study (Fig. S2).

### 2.3. Assessment of morphological parameters in broccoli sprouts exposed to MNPs

Sprout growth parameters (fresh weight (g) and total length (cm)) were evaluated for each treatment group exposed to plastic particles. Twelve days after sowing, sprout length was measured from the base of the hypocotyl to the apical tip. Seedlings were subsequently scanned using the WinRHIZO Reg software (Regent Instruments Inc., Québec, Canada) to obtain detailed morphological information. After scanning, seedlings were manually divided into two parts: the radicle and the hypocotyl (aerial portion of the sprout). To remove any remaining substrate or plastic residues, radicles were rinsed three times with distilled water, air-dried for 24 h, and stored in labeled paper envelopes. Root morphological traits—including radicle length, surface area, mean diameter, and volume—were then quantified using WinRHIZO software. Six replicates were prepared per treatment.

### 2.4. Extraction and quantification of phytohormones in broccoli sprouts exposed to MNPs

Phytohormone extraction were assessed following Pan et al. 2010 [14], with modifications optimized for our laboratory conditions. For extraction, 0.5 g of ground tissue was placed in 15 mL tubes containing 10 mL of extraction solvent (2-propanol/$H_2O$/concentrated HCl, 2:1:0.002, v/v/v). Samples were shaken at 100 rpm for 30 min at 4 °C. Subsequently, 20 mL of dichloromethane was added, and tubes were shaken again for 30 min under the same conditions. The mixtures were then centrifuged at 13,000×*g* for 5 min at 4 °C to achieve phase separation. From the lower phase, 9 mL were carefully collected with a micropipette, transferred to a round-bottom flask, and evaporated to dryness by rotary evaporation at 40 °C. The residue was reconstituted in 4 mL of solvent, followed by the addition of 1 mL of methanol to obtain a final volume of 5 mL. The resulting solution was filtered through 0.22 μm PVDF syringe filters and transferred into vials for HPLC analysis. Six replicates were prepared per treatment (n = 6). The results were expressed as mg 100 $g^{-1}$.

### 2.5. Antioxidant response of sprouts exposed to microplastics: catalase (CAT) activity

Catalase (CAT) extraction and activity were assessed following Kalir et al. (1984) [15] and Badiani et al. (1990) [16], with modifications optimized for our laboratory conditions. The assay quantified the amount of $H_2O_2$ decomposed by CAT over a defined time interval. Freshly germinated tissue (0.5 g) was homogenized in 5 mL of 25 mM HEPES buffer (pH 7.8), filtered through four layers of gauze, and centrifuged at 11,500 rpm for 20 min. A 0.5 mL aliquot of the supernatant (enzyme extract) was then mixed with 0.75 mL of 25 mM sodium phosphate buffer ($Na_2HPO_4/NaH_2PO_4$, pH 7), 0.75 mL of 0.8 mM Na-EDTA, and 1 mL of $H_2O_2$ (nM). The mixture was gently agitated, and CAT activity was determined spectrophotometrically (Orion Aquamate 8000 UV-VIS Spectrophotometer) by recording the decrease in absorbance at 240 nm over 3 min, corresponding to $H_2O_2$ consumption in the reaction medium. Six replicates were prepared per treatment (n = 6). The results were expressed as μmol·$min^{-1}$·$g^{-1}$ FW.

### 2.6. Extraction of glucosinolates from broccoli sprouts exposed to MNPs

For glucosinolate extraction, 100 mg of freeze-dried broccoli sprout powder was mixed with 1 mL of 70% methanol (v/v). The samples were vortexed briefly and immediately placed in a thermostatically controlled water bath at 70 °C for 20 min. During incubation, the samples were agitated every 5–10 min using a vortex mixer to enhance compound extraction. After heating, the tubes were transferred to ice for 5 min to stop the extraction process. The samples were centrifuged at 3000 rpm for 30 min, and the supernatant was carefully collected. The extracts were filtered through a 0.22 μm PVDF membrane filter and transferred to amber vials for subsequent analysis by LC-MS.

### 2.7. Chromatographic Identification and quantification of glucosinolates

Glucosinolates were identified and quantified using HPLC-DAD-ESI-MSn (Agilent Technologies, Waldbronn, Germany), based on their UV–Vis absorption spectra, retention times, and characteristic fragmentation patterns (MS and $MS^n$), following the protocol described by Baenas et al. (2016) [17]. Chromatograms were acquired at 227 nm, and quantification was achieved using glucoerucin and glucobrassicin as external standards for aliphatic and indolic glucosinolates, respectively (Sigma-Aldrich, St. Louis, MO, USA). All analyses were conducted in sextuplicate, and the results were expressed as mg per 100 g dry weight (DW).

### 2.8. Extraction and quantification of phenolic compounds from broccoli sprouts exposed to MNPs

For the extraction and quantification of phenolic compounds, 100 mg of freeze-dried plant material was used per sample. Extraction was performed using 1 mL of a solvent mixture (25:1:24, v/v/v) composed of methanol, water, and formic acid. Samples were first vortexed to homogenize the material, then subjected to ultrasonication for 1 h, followed by 24 h of extraction at 4 °C. After extraction, the samples were vortexed again to ensure uniformity and centrifuged at 3000 rpm for 30 min. The supernatant was carefully collected and filtered through a 0.22 μm PVDF membrane (Millex V13, Millipore, Bedford, MA, USA), and the final extracts were stored in amber vials for subsequent chromatographic analysis. All solvents used for extraction were of analytical grade and obtained from Merck (Darmstadt, Germany).

Phenolic profiles were determined using an Agilent HPLC 1100 series system equipped with a photodiode array detector and a tandem mass spectrometer (Agilent Technologies, Waldbronn, Germany). The system included a binary pump (model G1312A), autosampler (model G1313A), degasser (model G1322A), and photodiode array detector (model G1315B), all operated with ChemStation software (Agilent, version 08.03). Chromatographic separation was performed on a Luna C18 column (250 × 4.6 mm, 5 μm, 100 Å; Phenomenex, Torrens, CA, USA), protected with Security Guard Cartridges PFD C18 (4 × 3.0 mm). The mobile phases were deionized water/formic acid (99:1, v/v; phase A) and methanol (phase B). The flow rate was set to 0.9 mL/min with an injection volume of 20 μL.

Mass detection was carried out with an ion trap spectrometer (model G2445A) equipped with an electrospray ionization (ESI) interface and controlled by LCMSD software (Agilent, version 4.1). The optimized ionization parameters were capillary temperature 350 °C, voltage 4 kV, nebulizer pressure 65 psi, and nitrogen flow 11 L/min. Full-scan spectra were recorded across an *m/z* range of 100–1200. Collision-induced fragmentation was performed in the ion trap using helium as the collision gas with voltages ramped from 0.3 to 2 V.

Quantification was performed by external calibration with authentic standards freshly prepared each day p-coumaric acid (320 nm), (320 nm), quercetin-3-O-rutinoside (360 nm), cyanidin-3-O-glucoside (520 nm), and sinapic acid (320 nm). Six replicates were prepared per treatment (n = 6), and results were expressed as milligrams per 100 g of dry weight (mg 100 $g^{-1}$ dw).

### 2.9. Antioxidant capacity in sprouts exposed to MNPs

The oxygen radical absorbance capacity (ORAC-FL) assay [18] were used to measure free radical scavenging activity, with minor modifications. Analyses were performed in black 96-well microplates (Nunc, Roskilde, Denmark) using a Synergy H1 multimode microplate reader (BioTek, Winooski, VT, USA). Trolox was used as the calibration standard. In each well, 25 μL of sample extract, standard, or blank and 150

μL of fluorescein solution were added, and the plate was incubated at 37 °C for 30 min. The reaction was initiated by adding 25 μL of AAPH solution, and fluorescence was recorded every minute for 60 min at excitation and emission wavelengths of 485 nm and 520 nm, respectively. Antioxidant capacity was calculated from the difference in the area under the fluorescence decay curve between the sample and the blank. Results were expressed as mg Trolox equivalents per 100 g dry weight (mg TE 100 $g^{-1}$ DW), using six replicates.

### 2.10. Statistical and multivariate analyses of broccoli sprouts exposed to MNPs under varying environmental conditions

Biochemical and morphophysiological variables (glucosinolate profiles by subtype and totals; sinapic-derivative phenylpropanoids and anthocyanins—including totals; phytohormones IAA/$GA_3$/IBA; and dry weight) were analyzed with univariate inference such as Analysis of Variance (ANOVA) followed by Tukey's post hoc test was used; results were deemed significant at $\alpha = 0.05$ ($p < 0.05$) and were computed in R (v4.0.5). To evaluate the effects of the experimental factors—microplastic type, $CO_2$ concentration, and temperature— on plant biochemical and physiological variables, we implemented a multivariate statistical and predictive-modeling framework in R (v4.0.5). Correlation analysis was first conducted by computing a Pearson correlation matrix between bioactive compounds (individual and total glucosinolates, phenolics, sinapate derivatives, and phytohormones) and physiological parameters (dry weight), an exploratory step that characterized linear associations among variables and informed subsequent dimensionality reduction. Principal Component Analysis (PCA) was then performed on mean-centered data to summarize multivariate variability and reduce redundancy; principal components were retained based on explained variance and inspection of the scree plot, biplots were generated to visualize variable contributions, and the first six components were selected for downstream analyses. Assumption checks preceded parametric modeling: multivariate normality was assessed with Mardia's test, where skewness ($p = 0.38$) indicated no serious departure while kurtosis ($p = 0.047$) suggested mildly heavier tails; accordingly, although strict multivariate normality was not fully met, we proceeded with Multivariate Analysis of Variance (MANOVA) using Pillai's trace criterion given its robustness under modest assumption violations, treating the first six principal components as dependent variables to test the effects of the experimental factors on the principal dimensions of the system. Artificial Neural Network (ANN) modeling was finally employed via a multilayer perceptron with three input variables (microplastic type, $CO_2$, and temperature), three fully connected hidden layers, and six output nodes corresponding to the selected principal components; training was carried out using backpropagation, and predictive performance was quantified with root-mean-square error (RMSE) and the coefficient of determination ($R^2$).

The use of PCA-derived components as neural network outputs was motivated by both statistical and biological considerations. The multivariate structure of the dataset, characterized by strong correlations among hormonal, morphological, and phytochemical variables, creates redundancy that can hinder direct prediction of raw variables and increase the risk of overfitting. PCA offers an orthogonal transformation that captures the major latent physiological axes underlying the dataset, effectively condensing high-dimensional information into independent components that represent coherent biological processes rather than isolated measurements. Using these components as neural network outputs therefore allows the model to learn patterns associated with integrated physiological states, improving stability, reducing noise sensitivity, and enhancing generalization relative to predicting individual variables.

From a modeling perspective, the choice of a neural network was justified by the nonlinear and interactive structure of the data. Plant responses to combined $CO_2$, temperature, and microplastic exposures do not follow simple additive relationships, and preliminary tests indicated that linear regressions and traditional machine-learning alternatives (e.g., decision trees, Random Forest, Support Vector Machines) were less capable of capturing the multidimensional, nonlinear behavior of the system. Neural networks, in contrast, demonstrated superior adaptability to complex interactions and provided the highest predictive accuracy for the latent physiological axes derived from PCA. By predicting these integrated components rather than raw variables, the network could better reflect the true multivariate nature of plant responses while preventing dimensionality-driven overfitting. Thus, the combined PCA–NN framework offered a biologically grounded, mathematically robust, and computationally efficient approach for modeling emergent physiological states in broccoli sprouts under simultaneous pollutant and climate stressors.

## 3. Results and discusion

### 3.1. Morphological response to combined stressors

Assessing $CO_2$ × Temperature treatments, the impact of MNPs was most pronounced in hypocotyl traits (Fig. S3). The radicle length remained unaffected indicating that the harvested biomass (yield) was not linked to axial root elongation. At 500 ppm $CO_2$/20 °C, fresh weight increased under PE compared with PS or WP, while sprout length (hypocotyl + cotyledon) and dry weight showed only minor variations. At 1000 ppm $CO_2$/20 °C, PS reduced dry weight relative to PE, with WP showing intermediate values and no clear effects on fresh weight or sprout length. Under elevated temperature (28 °C), plastics appeared to buffer heat stress. At 28 °C, PS—and to a lesser extent PE—supported shoot biomass relative to WP (fresh weight: +56.6 % at 500 ppm and +30.1 % at 1000 ppm $CO_2$; dry weight at 1000 ppm: +16.7 %), while PE was generally intermediate. At 20 °C, differences were smaller and not always consistent across $CO_2$ levels. Fresh weight responded more strongly than dry weight, and root length showed no consistent plastic-specific pattern (Fig. S3), indicating that plastic effects were primarily linked to hypocotyl allocation and/or water relations rather than root foraging.

These results are consistent with reports showing that plant responses to MPs can be neutral or even transiently positive, largely due to changes in substrate physical properties (e.g., porosity, evaporation, water retention) rather than direct particle toxicity [19–21]. Indeed, non-degradable polymers such as PE and PS often elicit heterogeneous outcomes depending on particle type, size, concentration, soil texture, and exposure duration [22,23]. In Brassicaceae sprouts, LDPE has been shown to induce dose-dependent effects on biomass and secondary metabolites such as glucosinolates, with neutral or positive outcomes at low doses but predominantly negative responses at medium to high levels. Symplastic transport of aggregated MPs has been demonstrated in rapeseed [24], while in pak-choi, PE (virgin and aged) exhibited dose- and stage-specific effects, altering growth traits [25]. Previous works support the interpretation that the short-term thermal buffering observed here reflects substrate-mediated physical effects, whereas higher doses, prolonged exposure, or greater system complexity often shift the balance toward adverse outcomes for plant physiology and soil biota. Within this framework, the morphological patterns across $CO_2$–temperature regimes indicate that biomass allocation is primarily shaped by the thermal environment, with MNPs functioning as secondary modulators that fine-tune growth rather than drive it. The reduced elongation under heat aligns with the hormonal and metabolic signatures of stress described in later sections, suggesting a coordinated slowdown of primary growth processes when sprouts face simultaneous pollutant and climate pressures.

### 3.2. Phytohormonal signaling (IAA, $GA_3$, IBA)

Phytohormonal profiles revealed that indole-3-acetic acid (IAA) remained relatively stable across treatments and environments

(0.19–0.49 μg $g^{-1}$ DW; Fig. 1), with only minor, non-systematic fluctuations. This stability is in line with previous reports showing context-dependent auxin responses, while warming can enhance auxin levels and signaling in Arabidopsis seedlings (e.g., 28 °C vs. 20 °C) [26], in broccoli sprouts, temperature, rather than $CO_2$, appears to exert a stronger influence on hormonal composition, including IAA [27]. In contrast, gibberellic acid ($GA_3$) exhibited the clearest environment × polymer interaction, with mean concentrations peaking at 14.6 μg $g^{-1}$ DW under PS at 1000 ppm $CO_2$/20 °C, compared to 11.7 μg $g^{-1}$ in WP and 7.4 μg $g^{-1}$ in PE. Under heat (28 °C), $GA_3$ declined to ≈ 7–10 μg $g^{-1}$ DW (−30–40 %), confirming thermal repression of GA biosynthesis. This agrees with evidence that heat stress suppresses GA production and signaling, and that fine-tuning GA pathways is key for thermotolerance [28]. The effects of elevated $CO_2$ ($eCO_2$) were moderate and context-dependent—enhancing $GA_3$ at 20 °C but not at 28 °C—consistent with studies showing that $eCO_2$ can reconfigure hormonal pathways, including auxins and gibberellins, in a species- and tissue-specific manner [29] and promote GA/auxin-mediated adjustments of root growth [30]. Indole-3-butyric acid (IBA) remained at low concentrations (0.006–0.041 μg $g^{-1}$ DW) without significant variation across conditions (Fig. 1), which is plausible given that under low-to-moderate stress, hormonal signaling is often preserved and microplastic-induced shifts are subtle [31]. Altogether, these quantitative patterns highlight temperature as the dominant regulator of hormonal balance, particularly $GA_3$, while $CO_2$ and microplastics function as secondary modulators with strongly environment-dependent effects. The hormonal adjustments closely mirror the morphological outcomes: elevated $CO_2$ enhances auxin- and gibberellin-associated growth signals under moderate temperatures, whereas heat suppresses them regardless of MNP presence. This alignment with the reduced biomass observed at high temperature reinforces the interpretation that MNPs modulate, rather than override, the overarching $CO_2$–temperature framework that governs sprout hormonal dynamics.

It is important to point out that hormonal profiling in this study was deliberately focused on growth-related phytohormones to capture early developmental responses. While stress-associated hormones such as ABA, JA, and SA are undoubtedly relevant under multistressor scenarios, their inclusion would provide additional mechanistic resolution and is proposed for future transcriptomic and hormone-targeted studies.

### 3.3. Antioxidant enzyme activity (catalase) in broccoli sprouts

Catalase (CAT) activity showed no significant differences among polyethylene (PE), polystyrene (PS), and the without-plastic control (WP) across environments (Fig. S4). Absolute activities were moderate, with no differences between treatments by environment (~1.48–17.02 μmol $min^{-1}·g^{-1}$ FW). Temperature exerted a stronger influence than polymer type (mean CAT activity at 20 °C, at 500 and 1000 ppm $CO_2$) exceeded the corresponding values at 28 °C, with the most pronounced decline under PE. Shifts associated with elevated $CO_2$ were minor and inconsistent. In general, CAT activity did not differentiate between MPs treatments at the sampling time, and its modulation was primarily driven by temperature rather than $CO_2$ [32–35]. In this study, we prioritized CAT activity as an enzymatic marker of $H_2O_2$ detoxification because of its very high catalytic capacity and central peroxisomal role during germination and early Brassica growth. As a high-throughput route for $H_2O_2$ removal, CAT offers a robust readout of ROS balance in seedlings and is less susceptible than peroxidase-based pathways to transient inhibition or fluctuations in reductant supply. However, the limited variation in CAT activity observed here—particularly under heat—suggests that sprouts may rely on alternative antioxidant pathways or transient ROS-buffering mechanisms rather than sustained CAT activation. When viewed alongside the hormonal reductions and morphological constraints imposed by high temperature, these patterns point toward a stress-response configuration dominated by metabolic reallocation rather than strong enzymatic detoxification.

Hence, in future works gene-level validation of key regulatory pathways, including MYB- and CYP-associated genes, represents a logical next step to further resolve the molecular mechanisms underlying the observed metabolic responses.

### 3.4. Bioactive compounds in broccoli sprouts exposed to micro/nanoplastics

#### 3.4.1. Glucosinolates

Temperature emerged as the main determinant of glucosinolate accumulation in sprouts (mg 100 $g^{-1}$ DW). Across $CO_2$ regimes, raising the temperature from 20 to 28 °C nearly doubled glucosinolate levels (≈1000–1200 vs. ≈500–800 mg 100 $g^{-1}$ DW) (Table 1). By contrast, increasing $CO_2$ from 500 to 1000 ppm produced only modest effects: at 20 °C concentrations were slightly lower at 1000 ppm, whereas at 28 °C $CO_2$ exerted no significant influence. The role of MPs was minor and environment dependent. A treatment contrast was detected only under 500 ppm $CO_2$/20 °C, where PE plants accumulated more glucosinolates than WP (PS intermediate). In all other conditions, polymer identity did not differentiate responses. In general, warming strongly enhanced

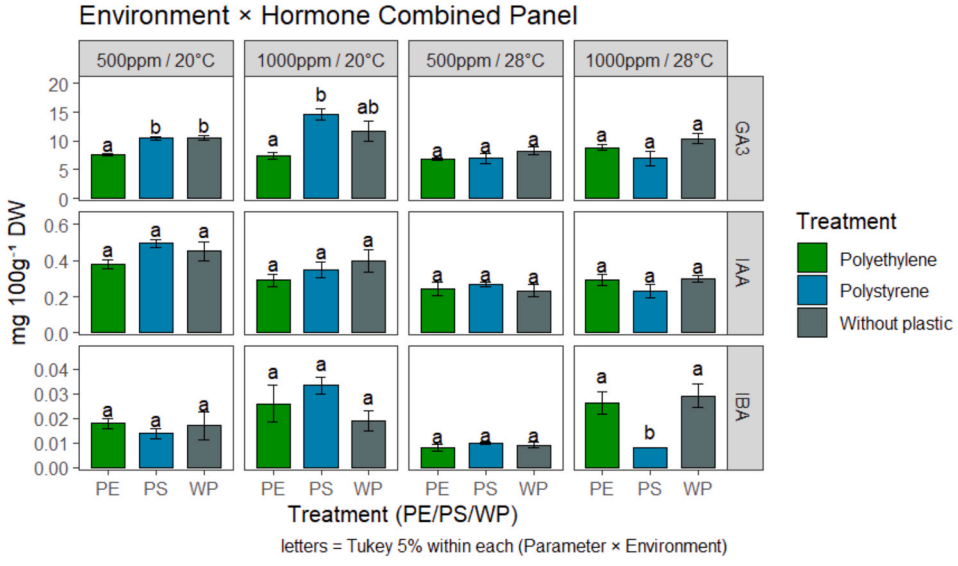


**Fig. 1.** Changes in phytohormone concentrations under varying environmental conditions.

**Table 1**
Glucosinolate content by environment and polymer in broccoli sprouts (mg 100 $g^{-1}$ DW).

| | Temperature = 20 °C | | | | | | Temperature = 28 °C | | | | | |
|---|---|---|---|---|---|---|---|---|---|---|---|---|
| | $CO_2$ = 500 ppm | | | $CO_2$ = 1000 ppm | | | $CO_2$ = 500 ppm | | | $CO_2$ = 1000 ppm | | |
| ***GSL compounds*** | WP | PS | PE | WP | PS | PE | WP | PS | PE | WP | PS | PE |
| **GRA** | 122.7 ± 14.4a | 197.6 ± 44b | 208.1 ± 17.9b | 176.4 ± 26.9a | 134.5 ± 60.0a | 330.5 ± 44.1b | 303.5 ± 21.7b | 184 ± 69.3a | 147.4 ± 33.6b | 388.6 ± 11.9a | 327.1 ± 30a | 363.1 ± 10.3a |
| **HGB** | 59.7 ± 15.9a | 73.3 ± 22.3a | 71 ± 21.5a | 60.2 ± 3.1a | 70.9 ± 17.8a | 68.7 ± 7a | 92.3 ± 7.6a | 92.7 ± 24.9a | 58.9 ± 7.2a | 57.7 ± 7.4a | 63.4 ± 5.0a | 68.5 ± 11.9a |
| **GER** | 208 ± 21a | 246 ± 15a | 252 ± 42a | 162 ± 13a | 179 ± 20a | 202 ± 15a | 385 ± .44a | 540 ± 108a | 423 ± 74a | 306 ± 43a | 376 ± 94a | 292 ± 3a |
| **GBS** | 92.4 ± 12a | 94.5 ± 8.1a | 110.9 ± 9.6a | 89.5 ± 12.4a | 93.9 ± 6.2a | 76.4 ± 6.8a | 72.8 ± 7a | 109.9 ± 24.2a | 85.4 ± 9a | 62.8 ± 9a | 56.4 ± 7.8a | 72.1 ± 7.1a |
| **MGB** | 116.6 ± 7.1 ab | 108.8 ± 14.1a | 146.2 ± 19.4b | 78.8 ± 1.7a | 92.4 ± 13.9a | 95.9 ± 22.6a | 122.4 ± 8.9a | 164.6 ± 14b | 149.7 ± 22.8 ab | 144.2 ± 8.2a | 143.8 ± 22.7a | 139.5 ± 1.6a |
| ***Total GSL*** | 600 ± 51a | 720 ± 56 ab | 788 ± 89b | 567 ± 24a | 571 ± 104a | 773 ± 71b | 977 ± 60a | 1091 ± 234a | 864 ± 96a | 934 ± 96a | 982 ± 136a | 945 ± 9a |

WP: without plastic; PS: with polystyrene; PE: with polyethylene. Mean ± SE for six replications within each environment. Different letters mean significant differences at $p < 0.05$ in polymer treatments for broccoli sprouts analyzed within each environment according to Tukey test.

glucosinolate content, elevated $CO_2$ had at most a mild attenuating effect at 20 °C and a neutral effect at 28 °C, and microplastics exerted only secondary, context-specific influences.

Our results indicate that temperature is the primary determinant of glucosinolate content: at 28 °C, concentrations were consistently higher than at 20 °C, while the effects of $CO_2$ were weak or absent, and the presence of MPs (PE, PS, WP) acted as a secondary, environment-dependent factor (a single contrast PE > WP observed only under 500 ppm $CO_2$/20 °C). This pattern aligns with the literature reporting marked thermal sensitivity of the GSL pathway and class-/tissue-specific profile shifts, including increases under certain high-temperature conditions in cultivated Brassica [36,37], and cooling-specific modulations in other species [38,39]. Responses to elevated $CO_2$ are context-dependent: $CO_2$ enrichment can stimulate the pathway (e.g., in broccoli sprouts [40]; or attenuate it via nitrogen dilution and altered C/N balance [41], consistent with the lack of a robust $CO_2$ effect in our system. Finally, although reductions in GSL under microplastic exposure have been reported [42], along with metabolic alterations associated with particle uptake [43], the signal under our conditions was minimal, suggesting that, within the tested ranges, MPs did not durably reprogram GSL metabolism. Collectively, these findings indicate that warming dominates GSL homeostasis, whereas $CO_2$ and microplastics exert smaller and more context-dependent effects.

Beyond total amounts, the class balance shifted in a predictable way: at 28 °C all treatments converged to an aliphatic-dominant profile (~70:30 aliphatic:indolic) (Fig. 2), whereas at 20 °C the composition diverged, with PE showing a higher aliphatic share and PS retaining comparatively more indolics.

This pattern is consistent with a temperature, and redox-driven activation of the aliphatic branch (MYB28/MYB29) under warming, whereas cooler conditions maintain indolic signaling through MYB34/MYB51/MYB122 and its crosstalk with auxin. Polymer identity acted only as a weak modifier of this baseline. PE promoted sulfur-rich aliphatic allocation via physical effects on soil structure and water status, while PS aligned with a mild biotic-like/oxidative shift toward indolic metabolism [38,44–46]. In soils, microplastic influences typically arise from changes in porosity, aggregation, and water retention rather than strong chemical cues, which explains the small and environment-dependent contrasts observed here [19,20].

In synthesis, the phytochemical landscape shows strong temperature-driven restructuring, with glucosinolates acting as early-defense indicators that rise under moderate stress but diminish when heat intensifies physiological pressure. The interaction patterns parallel hormonal downregulation and growth suppression, reinforcing the view that heat imposes the dominant constraint, while MNPs exert context-dependent but comparatively subtler influences on sprout functional quality.

### *3.4.2. Phenolic compounds: anthocyanins and sinapic acid derivatives*

Across environments, anthocyanin concentrations showed limited sensitivity to polymer identity and $CO_2$ (Table 2). A single environment-specific effect was detected at 500 ppm $CO_2$/28 °C, where PS > WP, with PE intermediate, indicating a light polymer-dependent stimulation of anthocyanin accumulation under warming at ambient $CO_2$. At 20 °C (both $CO_2$ levels) and at 1000 ppm $CO_2$/28 °C, anthocyanin levels did not differ among PE, PS, and WP. Changes attributable to elevating $CO_2$ from 500 to 1000 ppm were small and unsystematic, whereas temperature effects were context dependent. Similarly, sinapic acid-derived phenylpropanoids remained statistically unchanged across the treatments (Table 3). These results indicate that, under the tested conditions, the phenylpropanoid pathway leading to anthocyanins provides a more sensitive readout to warming in combination with polymer exposure, whereas sinapic derivatives appear comparatively buffered, and $CO_2$ enrichment exerts only a minor modulatory effect.

The environment-specific panels indicated that anthocyanins varied little with polymer identity or $CO_2$, with a single environment-specific

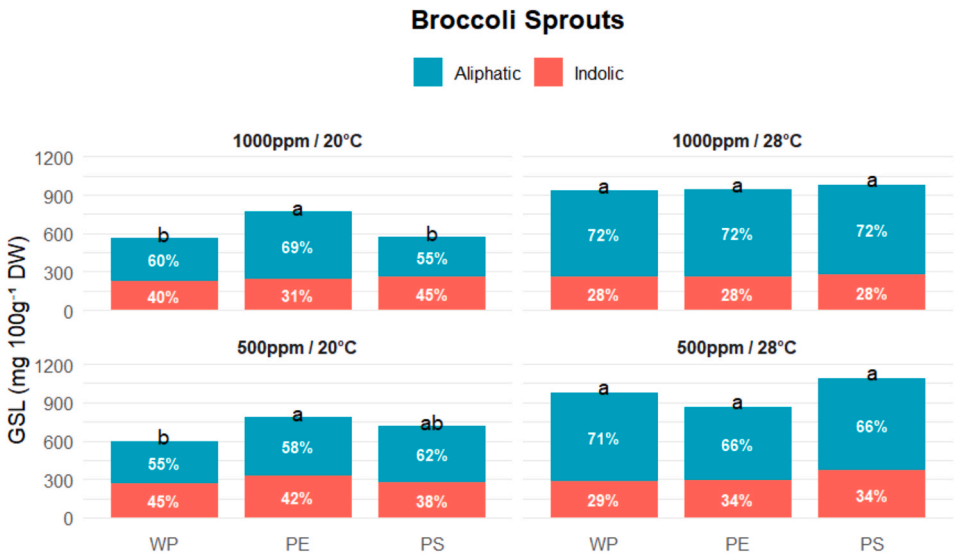


**Fig. 2.** Concentration of aliphatic and indolic glucosinolates under varying environmental conditions.

difference (PS > WP at 500 ppm $CO_2$/28 °C), whereas sinapic acid-derived phenylpropanoids remained statistically unchanged. This pattern is consistent with reports on broccoli, which showed that total anthocyanins are relatively heat-resilient, while higher temperatures increase other phenolics (including sinapic, ferulic, and *p*-coumaric acids), suggesting a redistribution of phenylpropanoid flux rather than a uniform decline in anthocyanins [47]. In kale, temperature has been shown to fine-tune the sinapate branch: disinapoyl-gentiobiose increases at higher temperatures, whereas lower temperatures favor complex sinapoyl-acylated flavonols, supporting the buffering effect observed here for total sinapates [48,49]. The effects of elevated $CO_2$ are generally context-dependent. Although $CO_2$ enrichment can stimulate phenolic accumulation or antioxidant capacity in Brassicaceae, responses are not uniform across tissues and conditions, consistent with the absence of a systematic $CO_2$ effect in our study [40,50]. Finally, while microplastic exposure can alter the phytochemical profile of Brassica sprouts, including shifts in anthocyanins, the direction and magnitude of the response depend on the dose, polymer type, and

**Table 2**
Anthocyanin composition by environment and polymer in broccoli sprouts (mg 100 $g^{-1}$ DW).

| *Anthocyanin compounds* | Temperature = 20 °C | | | | | | Temperature = 28 °C | | | | | |
|---|---|---|---|---|---|---|---|---|---|---|---|---|
| | $CO_2$ = 500 ppm | | | $CO_2$ = 1000 ppm | | | $CO_2$ = 500 ppm | | | $CO_2$ = 1000 ppm | | |
| | WP | PS | PE | WP | PS | PE | WP | PS | PE | WP | PS | PE |
| **Cy 1+2** | 0.0001 ± 0.0000a | 0.0004 ± 0.0001a | 0.0005 ± 0.0005a | 0.0002 ± 0.0001a | 0.0001 ± 0.0001a | 0.0002 ± 0.0000a | 0.0010 ± 0.0010b | 0.0031 ± 0.0002a | 0.0028 ± 0.0005a | 0.0020 ± 0.0004a | 0.0012 ± 0.0010a | 0.0013 ± 0.0002a |
| **Cy 3** | 0.0003 ± 0.0001a | 0.0002 ± 0.0001a | 0.0005 ± 0.0003a | 0.0008 ± 0.0007a | 0.0006 ± 0.0003a | 0.0008 ± 0.0002a | 0.0019 ± 0.0002b | 0.0036 ± 0.0002a | 0.0020 ± 0.0003b | 0.0016 ± 0.0010a | 0.0012 ± 0.0006a | 0.0008 ± 0.0001a |
| **Cy 4** | 0.0079 ± 0.0020a | 0.0087 ± 0.0001a | 0.0100 ± 0.0022a | 0.0096 ± 0.0022a | 0.0128 ± 0.0032a | 0.0140 ± 0.0054a | 0.0110 ± 0.0022a | 0.0117 ± 0.0009a | 0.0123 ± 0.0014a | 0.0086 ± 0.0002a | 0.0103 ± 0.0031a | 0.0083 ± 0.0009a |
| **Cy 5** | 0.0030 ± 0.0008a | 0.0036 ± 0.0006a | 0.0041 ± 0.0009a | 0.0042 ± 0.0012a | 0.0044 ± 0.0003a | 0.0053 ± 0.0012a | 0.0043 ± 0.0010a | 0.0059 ± 0.0002a | 0.0062 ± 0.0016a | 0.0040 ± 0.0013a | 0.0048 ± 0.0017a | 0.0033 ± 0.0005a |
| ***Total Anthocyanins*** | 0.0112 ± 0.0028a | 0.0129 ± 0.0009a | 0.0150 ± 0.0035a | 0.0148 ± 0.0034a | 0.0179 ± 0.0032a | 0.0204 ± 0.0065a | 0.0182 ± 0.0020a | 0.0243 ± 0.0012a | 0.0233 ± 0.0037a | 0.0162 ± 0.0030a | 0.0175 ± 0.0047a | 0.0136 ± 0.0012a |

WP: without plastic; PS: with polystyrene; PE: with polyethylene. Cy 1 and 2: Cy-3-(sinapoyl)diglc-5-glc + Cy-3-(feruloyl)dglc-5-glc; Cy 3: Cy-3-(p-coumaroyl)(sinapoyl)dglc-5-glc; Cy 4: Cy-3-(sinapoyl)(sinapoyl)dglc-5-glc; Cy 5: Cy-3-(sinapoyl)(sinapoyl)dglc-5(malonyl)glc. Mean ± SE for six replications within each environment. Different letters mean significant differences at $p < 0.05$ in polymer treatments for broccoli sprouts analyzed within each environment according to Tukey test

**Table 3**
Sinapics composition by environment and polymer in broccoli sprouts (mg 100 $g^{-1}$ DW).

| Sinapic compounds | Temperature = 20 °C | | | | | | Temperature = 28 °C | | | | | |
|---|---|---|---|---|---|---|---|---|---|---|---|---|
| | $CO_2$ = 500 ppm | | | $CO_2$ = 1000 ppm | | | $CO_2$ = 500 ppm | | | $CO_2$ = 1000 ppm | | |
| | WP | PS | PE | WP | PS | PE | WP | PS | PE | WP | PS | PE |
| **isorhmnt-3-sophtr-7-glc** | 0.016 ± 0.006a | 0.016± 0.004a | 0.017 ± 0.004a | 0.022 ± 0.001a | 0.027 ± 0.002b | 0.019 ± 0.004a | 0.022 ± 0.006a | 0.019 ± 0.001a | 0.016 ± 0.003a | 0.012 ± 0.001b | 0.019 ± 0.003c | 0.000 ± 0a |
| **kaempf-3-O-(p-coumaroyl)-soph-7-O-glc** | 0.207 ± 0.007a | 0.230± 0.027a | 0.255 ± 0.0180a | 0.142 ± 0.036a | 0.180 ± 0.004a | 0.180 ± 0.025a | 0.206 ± 0.017a | 0.225 ± 0.009a | 0.209 ± 0.019a | 0.204 ± 0.015a | 0.186 ± 0.035a | 0.188 ± 0.014a |
| **sinapylglucoside** | 3191.25± 385b | 418.16 ± 46a | 272.50 ± 26.a | 2855.77 ± 458a | 2977.22 ± 39a | 2626.97± 352a | 2569.25 ± 755b | 3517.80 ± 307b | 264.62 ± 97a | 171.74 ± 149a | 357.96 ± 82a | 332.99 ± 137a |
| **1,2-disinapoylgentiobioside** | 467.26 ± 44a | 528.43 ± 285a | 850.04 ± 284a | 764.52 ± 213b | 657.75 ± 114b | 235.76 ± 113a | 285.32 ± 92a | 1181.47 ± 336b | 192.06 ± 77a | 465.54 ± 294a | 2838.01 ± 2573a | 3801.25 ± 838a |
| **1-sinapoyl-2-feruloylgentiobiosido** | 733.09 ± 142b | 866.91 ± 62b | 193.03 ± 19a | 141.60 ± 18.b | 192.88 ± 27b | 621.17 ± 212a | 287.49 ± 143a | 570.34 ± 318a | 271.52 ± 41a | 270.77 ± 266a | 229.99 ± 94a | 130.88 ± 125a |
| **Unknown** | 1080.49 ± 327a | 248.88 ± 27b | 820.58 ± 257a | 859.26 ± 54a | 1053.50 ± 289a | 812.93 ± 184a | 314.78 ± 156a | 482.78 ± 160a | 279.92 ± 82a | 3012.60 ± 2829a | 359.23 ± 622a | 1074.79 ± 463a |
| **1,2,2'-trisinapoylgentiobioside** | 313.88 ± 45a | 862.41 ± 237b | 461.11 ± 103a | 252.70 ± 31a | 1118.42 ± 183a | 3672.23 ± 2505a | 320.77 ± 27b | 227.67 ± 86a | 160.87 ± 32a | 103.52 ± 92a | 1675.27 ± 1455a | 3308.50 ± 3667a |
| **1,2'-disinapoyl-2-feruloylgentibioside** | 5438.67 ± 79a | 5416.18 ± 313a | 5713.43± 842a | 4958.14 ± 672a | 4039.20 ± 2500a | 2077.24 ± 2686a | 5703.68 ± 1711b | 6225.15± 296b | 2251.99 ± 178a | 6480.04 ± 2537a | 1604.35 ± 1410a | 2561.98 ± 2579a |
| **Unknown** | 283.29 ± 38.a | 337.42 ± 31a | 4036.12 ± 3470a | 304.81 ± 78a | 257.73 ± 102a | 333.67 ± 112a | 298.06 ± 48b | 241.31 ± 88b | 8004.63± 182a | 209.07 ± 222a | 150.45 ± 137a | 181.94 ± 98a |
| **Total Sinapics** | 11507.96 ± 211a | 8678.42 ± 770a | 12346.84 ± 4172a | 10136.89 ± 883a | 10296.72 ± 2450a | 10380.01 ± 859a | 9779.38 ± 1411b | 12446.54 ± 796a | 11425.65 ± 238a | 10713.31 ± 4645a | 7215.29 ± 21229a | 11392.36 ± 1847a |

WP: without plastic; PS: with polystyrene; PE: with polyethylene. Mean ± SE for six replications within each environment. Different letters mean significant differences at $p < 0.05$ in polymer treatments for broccoli sprouts analyzed within each environment according to Tukey test.

developmental stage, such that small or null impacts, such as those observed here, are plausible under low-to-moderate stress [31,42]. Our results indicate that temperature acts as the dominant modulator of phenylpropanoid metabolism in Brassica sprouts, while $CO_2$ and microplastics function as secondary, strongly environment-dependent influencers. Under moderate stress conditions, sprouts appear to activate phenolic-based oxidative-defense pathways, but prolonged heat markedly restricts phenolic accumulation regardless of $CO_2$ or MNP exposure. This attenuation at elevated temperatures parallels the reductions in CAT activity and the hormonal suppression observed under heat, suggesting that secondary metabolism becomes deprioritized when thermal stress becomes the prevailing physiological constraint.

### 3.5. *Antioxidant capacity (ORAC) from broccoli sprouts exposed to micro/nanoplastics*

Total antioxidant capacity (ORAC; Fig. S5) was primarily shaped by temperature and its interaction with $CO_2$ and polymer identity. At 500 ppm $CO_2$/20 °C, treatments were statistically indistinguishable, whereas at 1000 ppm $CO_2$/20 °C, PE < PS (WP intermediate). Under 500 ppm $CO_2$/28 °C, WP < PE = PS, and at 1000 ppm $CO_2$/28 °C, PE exceeded PS (WP intermediate). These patterns indicate that warming generates context-dependent shifts in antioxidant potential: under elevated $CO_2$, PE and WP frequently recovered or exceeded their moderate-temperature values, while PS showed relative suppression. Because ORAC integrates phenolic contributions, these outcomes align with evidence that temperature reprograms phenylpropanoid allocation in Brassica—typically redistributing fluxes between hydroxycinnamates and flavonoids rather than uniformly modifying anthocyanins [31,40,42]. Elevated $CO_2$ can further enhance antioxidant capacity and bioactive metabolites in broccoli sprouts in a context-dependent manner, consistent with the PE and WP increases observed at 1000 ppm/28 °C. Modulation by microplastics is also coherent with reports showing MP-induced oxidative stress and variable antioxidant responses in Brassicaceae, particularly when polymer type, dose, and environmental conditions interact [47–49]. When integrated with the phenolic and hormonal patterns described above, ORAC values closely track the interplay between phenylpropanoid shifts, glucosinolate dynamics, and growth–defense trade-offs. Higher antioxidant capacity emerges under moderate stress, whereas heat imposes pronounced declines. This alignment between ORAC reductions, phenolic attenuation, and hormonal downregulation supports a unified interpretation: thermal stress exerts the dominant constraint on antioxidant potential, overshadowing the more context-dependent influence of MNPs.

These coordinated biochemical shifts not only clarify the physiological hierarchy imposed by temperature and $CO_2$, but also hold practical relevance for post-harvest valorization, as the extractability and stability of these metabolites depend strongly on their stress-induced profiles. High-temperature conditions enhanced certain phytochemical pools in sprouts, but these benefits can only be captured industrially if extraction approaches are compatible with thermosensitive metabolites. Recent advances show that microwave-assisted extraction (MAE) substantially increases extraction efficiency while reducing solvent use and processing time, although prolonged heating or excessive temperatures promote the degradation of labile compounds [51]. Likewise, water-induced complexation systems have emerged as a mild, solvent-reducing alternative capable of stabilizing carotenoids and pectins during extraction, demonstrating that bioactive–polymer interactions can enhance thermal stability and protect functional compounds during processing [52]. In practical terms, the patterns observed in our dataset indicate that sprouts grown under moderate stress—particularly under 20 °C conditions—maintain higher levels of glucosinolates, phenolics, and antioxidant capacity than those exposed to sustained heat. Such profiles are more compatible with advanced extraction technologies, which are sensitive to thermal degradation of bioactives. Therefore, moderately stressed sprouts may provide more suitable raw material for valorization platforms such as MAE or water-induced complexation, linking pre-harvest climate responses with post-harvest bioprocessing opportunities in the food industry.

### 3.6. *Multivariate analysis and predictive models*

Correlation analyses and PCA revealed a dominant axis (PC1) that opposed glucosinolates (Total GLs, glucoraphanin, and methoxyglucobrassicin) to growth hormones ($GA_3$ and IAA), with loadings of opposite sign and a negative association with dry weight (GL–DW correlations between −0.30 and −0.34) (Fig. 3). PC1 explained 32.1 % and PC2 17.4 % of the total variance, together capturing nearly half (49.5 %) of the multivariate structure. PC1 was dominated by total glucosinolates (loading = 0.93) and methoxyglucobrassicin (0.77) on the positive side,

in contrast to $GA_3$ (−0.79) and IAA (−0.74) on the negative side, confirming a clear antagonism between defense and growth metabolism. This pattern supports the interpretation that biomass decreases as chemical defense intensifies, consistent with the negative association of these hormones with dry weight (−0.34). Altogether, these results indicate a growth–defense trade-off, where allocation to defensive metabolites is favored at the expense of growth markers and biomass [53,54].

This multivariate pattern aligns with our univariate results, in which glucosinolates increased with temperature, whereas biomass and $GA_3$ tended to be depressed or decoupled from the defense profile, with evidence for cross-regulation between aliphatic/indolic MYBs and growth hormones in Brassicaceae [38,39]. Samples exposed to higher temperatures clustered toward the positive side of PC1—associated with defensive metabolism—while control or low-temperature plants were aligned on the negative side, characterized by higher $GA_3$, IAA, and biomass. A strong opposition between hormonal ($GA_3$, IAA) and defensive (total GLs, methoxyglucobrassicin) vectors was evident in the biplot (Fig. 4A), further illustrating the trade-off between growth and defense processes. PC2 separates glucobrassicin and sinapics (e.g., sinapyl glucoside, 1,2′-disinapoyl-2-feruloylgentiobioside) positively from glucoraphanin, reflecting a reorganization between indolic and aliphatic/sinapics pools (Fig. 4).

This is consistent with reports that warming and other stressors modulate phenylpropanoid and GL metabolism in a class-specific manner, with sinapates relatively dampened or redirected, and differential changes between indolic and aliphatic GLs [36,37,48,49]. Thus, the PC1–PC2 plane captures two interpretable biological dimensions, defense vs. growth and internal partitioning among GL/sinapate families. MANOVA (Table S2) confirms that PC1, the broadest physiological dimension, is sensitive to all three factors (MPs, $CO_2$, temperature), whereas PC2 and PC5 respond primarily to $CO_2$, and PC6 to micro/nanoplastics, validating at a latent scale what is observed at the trait level, temperature as a dominant modulator of the defense–growth axis (increased GLs, hormonal adjustment, and biomass changes), elevated $CO_2$ with light, context-dependent effects on specific pathways (phenylpropanoids and GL subclasses), and micro/nanoplastics with detectable but bounded impacts, especially on the component loading dry weight and IBA, consistent with mild physico-chemical microstress and fine, tuned growth adjustments. The negative loadings of $GA_3$ (−0.79) and IAA (−0.74) on PC1 and their vectorial opposition to GLs in the biplot support the interpretation that gibberellins and auxins antagonize GL accumulation under the evaluated scenarios. The literature shows that heat tends to attenuate GA signaling and readjust auxin homeostasis, favoring tolerance traits over vegetative expansion [26,28], consistent with the greater defense load concentrated by PC1 under warm conditions.

A neural-network model was trained using temperature, $CO_2$ concentration, and micro/nanoplastic exposure as input variables, and the first six principal components (PC1–PC6) as outputs (Fig. 5). This framework allowed us to evaluate how environmental and pollutant factors jointly predict the major axes of physiological and biochemical variation in broccoli sprouts. Model performance was highest for the leading components—PC1 to PC3 ($R^2$ = 94.4 %, 92.1 %, and 86.7 %; RMSE = 0.69, 0.60, and 0.63, respectively)—and declined for PC4–PC6 ($R^2$ = 59.4–83.7 %; RMSE = 0.58–0.89). These results indicate that most of the variability induced by temperature, $CO_2$, and MNPs is structured and predictable, yet exhibits nonlinear relationships that cannot be fully captured by traditional linear models. Importantly, the model demonstrates that environmental conditions—particularly temperature—can independently drive the main functional transitions in plants, such as the shift between growth and defense-oriented metabolism. Overall, the neural-network approach supports the use of machine-learning tools to anticipate integrated plant responses under complex global-change

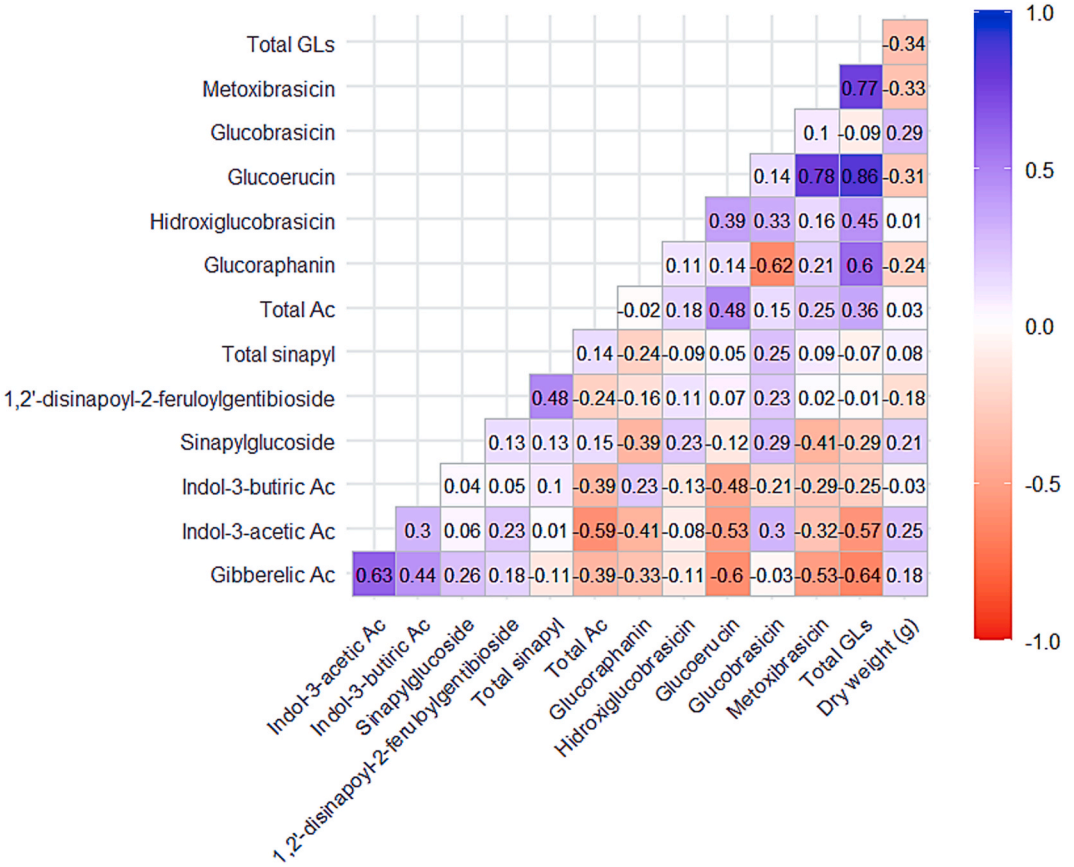


**Fig. 3.** Correlation matrix of glucosinolates, phytohormones, and biomass traits.

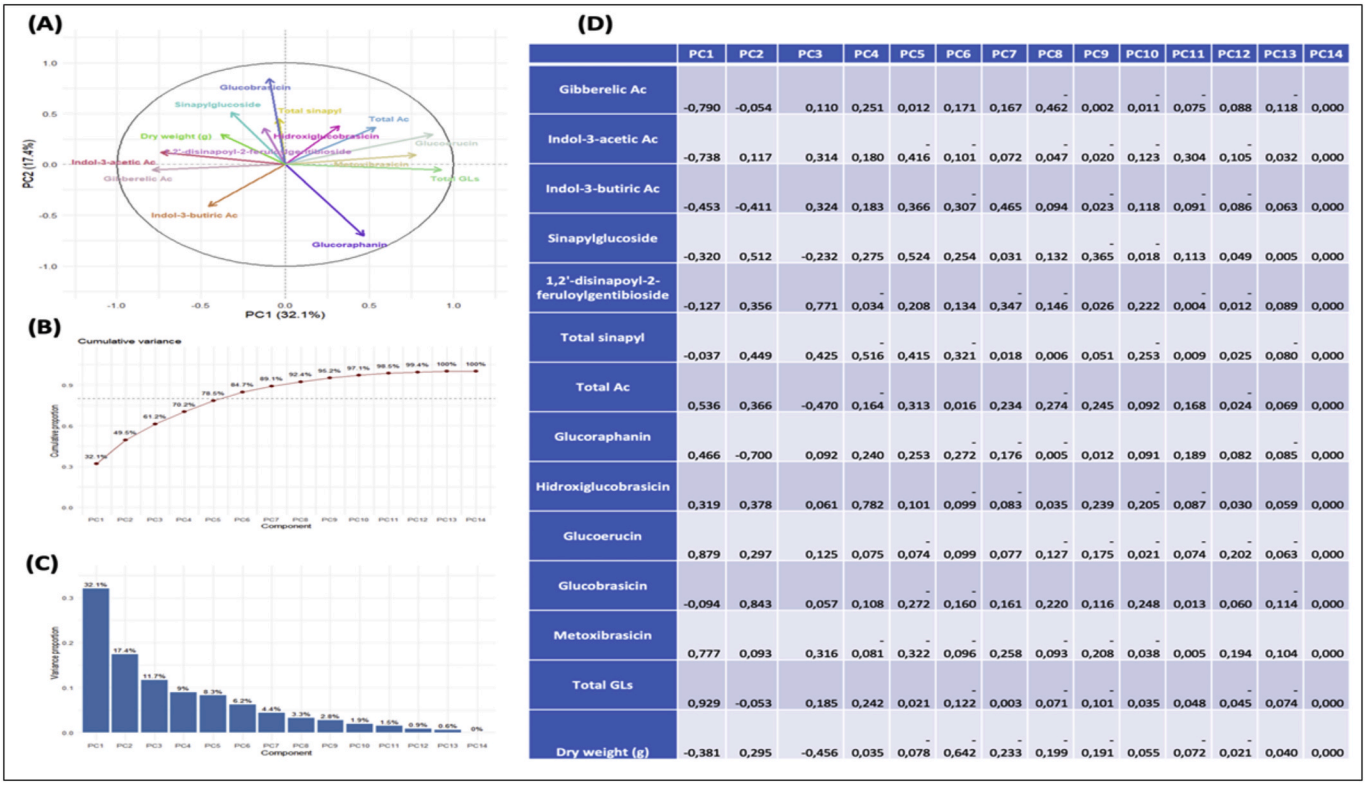


(D)

| | PC1 | PC2 | PC3 | PC4 | PC5 | PC6 | PC7 | PC8 | PC9 | PC10 | PC11 | PC12 | PC13 | PC14 |
|---|---|---|---|---|---|---|---|---|---|---|---|---|---|---|
| Gibberelic Ac | -0,790 | -0,054 | 0,110 | 0,251 | 0,012 | 0,171 | 0,167 | 0,462 | 0,002 | 0,011 | 0,075 | 0,088 | 0,118 | 0,000 |
| Indol-3-acetic Ac | -0,738 | 0,117 | 0,314 | 0,180 | 0,416 | 0,101 | 0,072 | 0,047 | 0,020 | 0,123 | 0,304 | 0,105 | 0,032 | 0,000 |
| Indol-3-butiric Ac | -0,453 | -0,411 | 0,324 | 0,183 | 0,366 | 0,307 | 0,465 | 0,094 | 0,023 | 0,118 | 0,091 | 0,086 | 0,063 | 0,000 |
| Sinapylglucoside | -0,320 | 0,512 | -0,232 | 0,275 | 0,524 | 0,254 | 0,031 | 0,132 | 0,365 | 0,018 | 0,113 | 0,049 | 0,005 | 0,000 |
| 1,2'-disinapoyl-2-feruloylgentibioside | -0,127 | 0,356 | 0,771 | 0,034 | 0,208 | 0,134 | 0,347 | 0,146 | 0,026 | 0,222 | 0,004 | 0,012 | 0,089 | 0,000 |
| Total sinapyl | -0,037 | 0,449 | 0,425 | 0,516 | 0,415 | 0,321 | 0,018 | 0,006 | 0,051 | 0,253 | 0,009 | 0,025 | 0,080 | 0,000 |
| Total Ac | 0,536 | 0,366 | -0,470 | 0,164 | 0,313 | 0,016 | 0,234 | 0,274 | 0,245 | 0,092 | 0,168 | 0,024 | 0,069 | 0,000 |
| Glucoraphanin | 0,466 | -0,700 | 0,092 | 0,240 | 0,253 | 0,272 | 0,176 | 0,005 | 0,012 | 0,091 | 0,189 | 0,082 | 0,085 | 0,000 |
| Hidroxiglucobrasicin | 0,319 | 0,378 | 0,061 | 0,782 | 0,101 | 0,099 | 0,083 | 0,035 | 0,239 | 0,205 | 0,087 | 0,030 | 0,059 | 0,000 |
| Glucoerucin | 0,879 | 0,297 | 0,125 | 0,075 | 0,074 | 0,099 | 0,077 | 0,127 | 0,175 | 0,021 | 0,074 | 0,202 | 0,063 | 0,000 |
| Glucobrasicin | -0,094 | 0,843 | 0,057 | 0,108 | 0,272 | 0,160 | 0,161 | 0,220 | 0,116 | 0,248 | 0,013 | 0,060 | 0,114 | 0,000 |
| Metoxibrasicin | 0,777 | 0,093 | 0,316 | 0,081 | 0,322 | 0,096 | 0,258 | 0,093 | 0,208 | 0,038 | 0,005 | 0,194 | 0,104 | 0,000 |
| Total GLs | 0,929 | -0,053 | 0,185 | 0,242 | 0,021 | 0,122 | 0,003 | 0,071 | 0,101 | 0,035 | 0,048 | 0,045 | 0,074 | 0,000 |
| Dry weight (g) | -0,381 | 0,295 | -0,456 | 0,035 | 0,078 | 0,642 | 0,233 | 0,199 | 0,191 | 0,055 | 0,072 | 0,021 | 0,040 | 0,000 |

**Fig. 4.** Principal component analysis (PCA) of glucosinolates, phytohormones, and plant biomass, (a) PCA biplot showing the distribution of traits across the first two principal components (PC1 and PC2), with arrows indicating the contribution of each variable, (b) Scree plot of the proportion of variance explained by each component, (c) Cumulative variance explained by successive PCs, showing that the first components account for most of the variation, (d) Loadings of each variable on the principal components, highlighting those with the strongest associations.

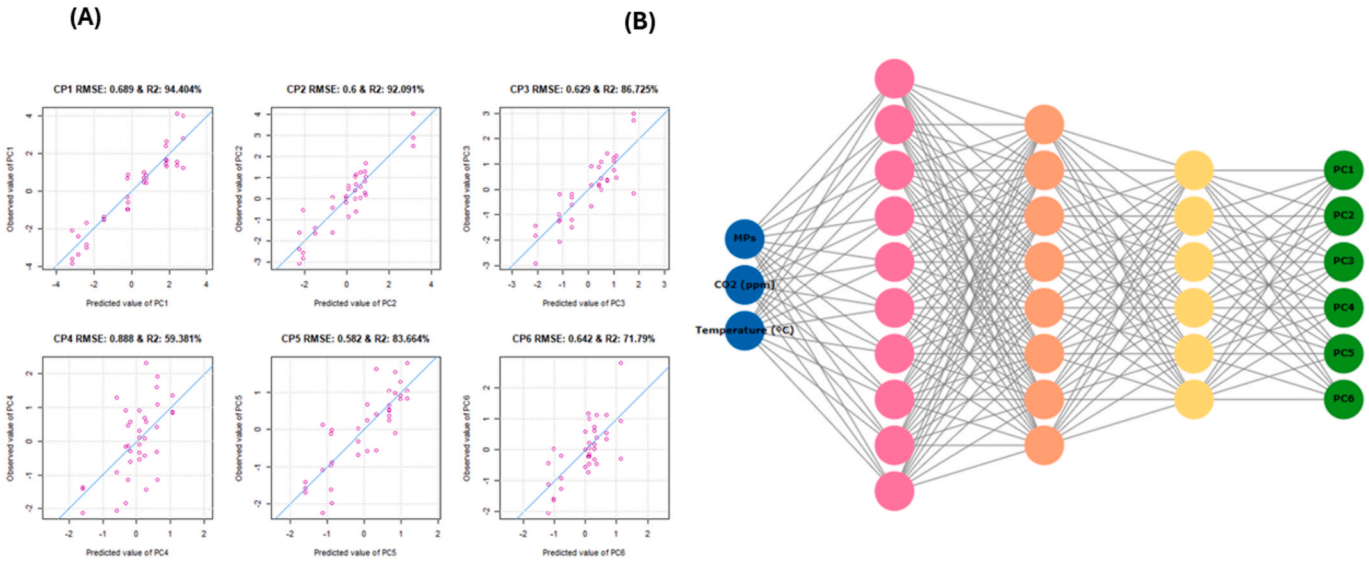


**Fig. 5.** Predictive modeling of PCA components using a neural network: architecture and model performance.

scenarios, highlighting that the leading latent axes (PC1–PC3) contain the most robust and biologically meaningful predictive signals [55–57] (Fig. 5).

In synthesis, the integration of correlations, PCA, MANOVA, and neural-network modeling converges on the view that warming reallocates resources from hormone-mediated growth toward sulfur-rich defenses and phenylpropanoids. Elevated $CO_2$ modulates subsets of pathways (notably PC2 and PC5) with effects dependent on nutritional context and tissue state, whereas microplastics induce measurable but secondary adjustments along the axis associated with biomass and IBA. Importantly, both multivariate and machine-learning models reveal that the balance between growth and defense in Brassicaceae does not occur randomly but rather emerges from complex yet predictable interactions between plant hormones and environmental cues. This multivariate reading, consistent with our prior univariate analyses, provides a mechanistic framework to interpret how climate-change factors and

pollutants jointly reconfigure growth–defense homeostasis in Brassicaceae.

In spite of biodegradable plastics (e.g., PBAT, PLA, PHA) were not evaluated in this study it is important to consider them. The available evidence indicates that these materials can elicit earlier [58] and more pronounced plant–soil responses than polyethylene or polystyrene [59], owing to the release of assimilable carbon and reactive degradation intermediates capable of restructuring the soil microbiome and modulating nitrogen availability [60–63]. Accordingly, our inferences should be regarded as conservative with respect to bioplastics. Future investigations should employ orthogonal experimental designs—crossing polymer chemistry with particle size/shape and climatic factors—to rigorously contrast the rapid bioactivity characteristic of biopolymers with the predominantly substrate-physical, short-term responses documented for PE/PS.

From an applied perspective, these results are relevant for broccoli sprout production systems, where early developmental stages are critical for functional quality. The absence of severe negative effects at the tested PE and PS concentrations suggests a low short-term risk for sprout-based food systems. Additionally, the modulation of bioactive compounds highlights opportunities for functional ingredient development under controlled growth conditions.

## 4. Conclusions

Temperature emerged as the dominant driver of broccoli sprout responses, enhancing glucosinolate biosynthesis while constraining biomass production. Elevated $CO_2$ exerted moderate and context-dependent effects, stimulating metabolic and hormonal activity under moderate conditions but losing its influence under heat stress. In contrast, micro- and nanoplastics acted as secondary modulators, subtly altering biomass and phenolic composition depending on the surrounding environment.

Glucosinolates behaved as early-defense markers, showing activation under moderate stress and attenuation under combined or severe conditions, reflecting a resource reallocation from defense to maintenance. Hormonal profiling revealed a $CO_2$- and temperature-dependent reconfiguration of gibberellin and auxin signaling consistent with the growth–defense balance. Together, these coordinated shifts across metabolic and hormonal networks underline the integrative nature of plant stress responses.

The joint action of $CO_2$ enrichment, elevated temperature, and microplastics resulted in predominantly antagonistic effects, where the stimulatory influence of $CO_2$ was offset by thermal and pollutant stress. Multivariate and neural-network analyses validated this pattern, confirming a temperature-centered hierarchy of regulation and highlighting the predictive power of machine-learning tools for disentangling complex environmental interactions.

This study advances a mechanistic understanding of how plants integrate multiple concurrent stressors in a climate-contaminant framework. Future research should couple physiological and omics-based approaches to elucidate how plastic particles intersect with hormonal and redox regulation, improving predictions of crop resilience under emerging global-change scenarios.

## 5. Glossary

MPs, microplastics; NPs, nanoplastics; MNPs, micro/nanoplastics; $eCO_2$, elevated carbon dioxide; PAR, photosynthetically active radiation; ROS, reactive oxygen species; UV, ultraviolet radiation; DW, dry weight; ppm, parts per million; WP, without plastic (control); PS, polystyrene; PE, polyethylene; HDPE, high-density polyethylene; PBAT, poly(butylene adipate-co-terephthalate); PLA, polylactic acid; PHA, polyhydroxyalkanoates; IAA, indole-3-acetic acid; GA, gibberellins; $GA_3$, gibberellic acid ($GA_3$); IBA, indole-3-butyric acid; CAT, catalase; GLs, glucosinolates; GRA, glucoraphanin; GER, glucoerucin; GBS, glucobrassicin; HGB, 4-hydroxyglucobrassicin; MGB, 4-methoxyglucobrassicin; HPLC, high-performance liquid chromatography; DAD, diode-array detector; ESI, electrospray ionization; MS, mass spectrometry; LC-MS, liquid chromatography–mass spectrometry; FTIR, Fourier-transform infrared spectroscopy; ORAC-FL, oxygen radical absorbance capacity (fluorescein); $H_2O_2$, hydrogen peroxide; ANOVA, analysis of variance; MANOVA, multivariate analysis of variance; PCA, principal component analysis; MLP, multilayer perceptron; RMSE, root-mean-square error; $R^2$, coefficient of determination.

## CRediT authorship contribution statement

**Marcelo Illanes:** Writing – original draft, Visualization, Resources, Investigation, Formal analysis, Conceptualization. **María Trinidad Toro:** Methodology, Formal analysis. **Felipe Noriega:** Methodology, Formal analysis. **Mauricio Schoebitz:** Writing – original draft, Visualization, Resources, Conceptualization. **Roberto Fustos-Toribio:** Methodology, Formal analysis. **Nelson Zapata:** Writing – original draft, Visualization, Resources, Conceptualization. **Diego A. Moreno:** Writing – review & editing, Resources, Methodology, Conceptualization. **María Dolores López-Belchí:** Writing – original draft, Visualization, Resources, Methodology, Investigation, Formal analysis, Conceptualization.

## Ethics statement

This study doesn't involve human and animal studies which require ethical approval.

## Declaration of generative AI and AI-assisted technologies in the manuscript preparation process

During the preparation of this work the author(s) used Scite and PaperPal in order to improve references and English grammar. After using these tools, the authors reviewed and edited the content as needed and take full responsibility for the content of the published article.

## Funding

This work has been supported by FONDECYT REGULAR project 1240947 and 1220425 (Agencia Nacional de Investigación y Desarrollo, ANID, Chile) and Doctoral Grants No 21210260 (Agencia Nacional de Investigación y Desarrollo, ANID).

This work was partly supported by the AGROALNEXT Program, granted by MCIN (Agroalnext_2022_027, "Hortnext"), NextGeneration EU (PRTR-C17.I1), and the Generalitat Valenciana.

## Declaration of competing interest

The authors declare that they have no known competing financial interests or personal relationships that could have appeared to influence the work reported in this paper.

## Acknowledgment

Recognition and gratitude to Doctoral Program in Agronomy Science at University of Concepción (UDEC), Chile.

## Appendix A. Supplementary data

Supplementary data to this article can be found online at https://doi.org/10.1016/j.jafr.2026.102724.

## Data availability

Data will be made available on request.

## References


[1] M. Illanes, M.-T. Toro, M. Schoebitz, N. Zapata, D.A. Moreno, M.D. López-Belchí, Integrating microplastic research in sustainable agriculture: challenges and future directions for food production, Curr Plant Biol 42 (2025) 100458, https://doi.org/10.1016/j.cpb.2025.100458.

[2] S. Sharma, V. Sharma, S. Chatterjee, Contribution of plastic and microplastic to global climate change and their conjoining impacts on the environment - a review, Sci. Total Environ. 875 (2023) 162627, https://doi.org/10.1016/j.scitotenv.2023.162627.

[3] R. Zhu, Z. Zhang, N. Zhang, H. Zhong, F. Zhou, X. Zhang, C. Liu, Y. Huang, Y. Yuan, Y. Wang, C. Li, H. Shi, M.C. Rillig, F. Dang, H. Ren, Y. Zhang, B. Xing, A global estimate of multiecosystem photosynthesis losses under microplastic pollution, Proc. Natl. Acad. Sci. 122 (11) (2025), https://doi.org/10.1073/pnas.2423957122.

[4] G.G.H.M. Gamage, N.H. Mudannayake, M. Premaratne, H.M.S.P. Madawala, Effect of microplastics on rhizosphere and arbuscular mycorrhizal fungi of <Em>Zea mays</Em&gt, Ceylon J. Sci. 54 (3) (2025) 855–864, https://doi.org/10.4038/cjs.v54i3.8944.

[5] A.L. Dawson, S. Kawaguchi, C.K. King, K.A. Townsend, R. King, W.M. Huston, S. M. Bengtson Nash, Turning microplastics into nanoplastics through digestive fragmentation by antarctic krill, Nat. Commun. 9 (1) (2018) 1001, https://doi.org/10.1038/s41467-018-03465-9.

[6] A. Murray, B. Örmeci, Removal effectiveness of nanoplastics (<400 nm) with separation processes used for water and wastewater treatment, Water (Basel) 12 (3) (2020) 635, https://doi.org/10.3390/w12030635.

[7] S. Li, T. Wang, J. Guo, Y. Dong, Z. Wang, L. Gong, X. Li, Polystyrene microplastics disturb the redox homeostasis, carbohydrate metabolism and phytohormone regulatory network in barley, J. Hazard. Mater. 415 (2021) 125614, https://doi.org/10.1016/j.jhazmat.2021.125614.

[8] M. Yamaguchi, N. Tazoe, T. Nakayama, T. Yonekura, T. Izuta, Y. Kohno, Combined effects of elevated air temperature and CO2 on growth, yield, and yield components of Japonica rice (Oryza Sativa L.), Asian J. Atmosph. Environ. 17 (1) (2023) 17, https://doi.org/10.1007/s44273-023-00019-4.

[9] S. Fortunato, C. Lasorella, N. Dipierro, F. Vita, M.C. de Pinto, Redox signaling in plant heat stress response, Antioxidants 12 (3) (2023) 605, https://doi.org/10.3390/antiox12030605.

[10] C.M. Galanakis, The food systems in the era of the coronavirus (COVID-19) pandemic crisis, Foods 9 (4) (2020) 523, https://doi.org/10.3390/foods9040523.

[11] C.M. Galanakis, The "Vertigo" of the food sector within the triangle of climate change, the post-pandemic world, and the Russian-Ukrainian War, Foods 12 (4) (2023) 721, https://doi.org/10.3390/foods12040721.

[12] C.M. Galanakis, The future of food, Foods 13 (4) (2024) 506, https://doi.org/10.3390/foods13040506.

[13] M.D. López, M.T. Toro, G. Riveros, M. Illanes, F. Noriega, M. Schoebitz, C. García-Viguera, D.A. Moreno, Brassica sprouts exposed to microplastics: effects on phytochemical constituents, Sci. Total Environ. 823 (2022) 153796, https://doi.org/10.1016/j.scitotenv.2022.153796.

[14] X. Pan, R. Welti, X. Wang, Quantitative analysis of major plant hormones in crude plant extracts by high-performance liquid chromatography-mass spectrometry, Nat. Protoc. 5 (6) (2010) 986–992, https://doi.org/10.1038/nprot.2010.37.

[15] Kair, A.; Omri, G.; Poljakoff-Mayber Kalir, A. Peroxidase and Catalase Activity in Leaves of Halimione Portidacoides Exposed to Salinity.

[16] M. Badiani, M.G. De Biasi, M. Colognola, F. Catalase Artemi, Peroxidase and Superoxide Dismutase Activities in Seedlings Submitted to Increasing Water Deficit *, 1990.

[17] N. Baenas, D. Villaño, C. García-Viguera, D.A. Moreno, Optimizing elicitation and seed priming to enrich broccoli and radish sprouts in glucosinolates, Food Chem. 204 (2016) 314–319, https://doi.org/10.1016/j.foodchem.2016.02.144.

[18] F. Noriega, C. Mardones, S. Fischer, C. Garciá-Viguera, D.A. Moreno, M.D. López, Seasonal changes in white strawberry: effect on aroma, phenolic compounds and its biological activity, J. Berry Res. 11 (1) (2021) 103–118, https://doi.org/10.3233/JBR-200585.

[19] A.A. De Souza Machado, C.W. Lau, W. Kloas, J. Bergmann, J.B. Bachelier, E. Faltin, R. Becker, A.S. Görlich, M.C. Rillig, Microplastics can change soil properties and affect plant performance, Environ. Sci. Technol. 53 (10) (2019) 6044–6052, https://doi.org/10.1021/acs.est.9b01339.

[20] M.C. Rillig, A. Lehmann, A.A. de Souza Machado, G. Yang, Microplastic Effects on Plants. New Phytologist, Blackwell Publishing Ltd, August 1, 2019, pp. 1066–1070, https://doi.org/10.1111/nph.15794.

[21] Y.M. Lozano, M.C. Rillig, Effects of microplastic fibers and drought on plant communities, Environ. Sci. Technol. 54 (10) (2020) 6166–6173, https://doi.org/10.1021/acs.est.0c01051.

[22] J. Zhou, Y. Wen, M.R. Marshall, J. Zhao, H. Gui, Y. Yang, Z. Zeng, D.L. Jones, H. Zang, Microplastics as an emerging threat to plant and soil health in agroecosystems, Sci. Total Environ. 15 (2021), https://doi.org/10.1016/j.scitotenv.2021.147444. Elsevier B.V. September.

[23] M. Sajjad, Q. Huang, S. Khan, M.A. Khan, Y. Liu, J. Wang, F. Lian, Q. Wang, G. Guo, Microplastics in the soil environment: a critical review, Environ. Technol. Innov. (2022), https://doi.org/10.1016/j.eti.2022.102408. Elsevier B.V. August 1.

[24] S. Rong, S. Wang, H. Liu, Y. Li, J. Huang, W. Wang, B. Han, S. Su, W. Liu, Evidence for the transportation of aggregated microplastics in the symplast pathway of oilseed rape roots and their impact on plant growth, Sci. Total Environ. 912 (2024), https://doi.org/10.1016/j.scitotenv.2023.169419.

[25] C. Men, Z. Xie, K. Li, X. Xing, Z. Li, J. Zuo, Single and combined effect of polyethylene microplastics (Virgin and naturally aged) and cadmium on pakchoi (Brassica Rapa Subsp. Chinensis) under different growth stages, Sci. Total Environ. 951 (2024), https://doi.org/10.1016/j.scitotenv.2024.175602.

[26] W.M. Gray, A. Anders Andersöstin, G. Göran Sandberg, C.P. Romano, M. Estelle, High Temperature Promotes Auxin-Mediated Hypocotyl Elongation in Arabidopsis, vol. 95, 1998. www.pnas.org.

[27] I. Šola, D. Gmižić, M. Pinterić, A. Tot, J. Ludwig-Müller, Adjustments of the phytochemical profile of broccoli to low and high growing temperatures: implications for the bioactivity of its extracts, Int. J. Mol. Sci. 25 (7) (2024), https://doi.org/10.3390/ijms25073677.

[28] S. Nagar, V.P. Singh, A. Arora, R. Dhakar, N. Singh, G.P. Singh, S. Meena, S. Kumar, R. Shiv Ramakrishnan, Understanding the role of gibberellic acid and paclobutrazol in terminal heat stress tolerance in wheat, Front. Plant Sci. 12 (2021), https://doi.org/10.3389/fpls.2021.692252.

[29] Y. Zhou, S. Ge, L. Jin, K. Yao, Y. Wang, X. Wu, J. Zhou, X. Xia, K. Shi, C.H. Foyer, J. Yu, A novel CO2-Responsive systemic signaling pathway controlling plant mycorrhizal symbiosis, New Phytol. 224 (1) (2019) 106–116, https://doi.org/10.1111/nph.15917.

[30] T. Hachiya, D. Sugiura, M. Kojima, S. Sato, S. Yanagisawa, H. Sakakibara, I. Terashima, K. Noguchi, High CO2 triggers preferential root growth of Arabidopsis thaliana via two distinct systems under low PH and low N stresses, Plant Cell Physiol. 55 (2) (2014) 269–280, https://doi.org/10.1093/pcp/pcu001.

[31] L. Jia, L. Liu, Y. Zhang, W. Fu, X. Liu, Q. Wang, M. Tanveer, L. Huang, Microplastic stress in plants: effects on plant growth and their remediations. Frontiers in Plant Science, Frontiers Media SA, 2023, https://doi.org/10.3389/fpls.2023.1226484.

[32] A. Mhamdi, G. Queval, S. Chaouch, S. Vanderauwera, F. Van Breusegem, G. Noctor, Catalase function in plants: a focus on arabidopsis mutants as stress-mimic models, in: Journal of Experimental Botany, Oxford University Press, 2010, https://doi.org/10.1093/jxb/erq282, 4197–4220.

[33] L.A. Del Río, L.M. Sandalio, F.J. Corpas, J.M. Palma, J.B. Barroso, Reactive oxygen species and reactive nitrogen species in peroxisomes. Production, scavenging, and role in cell signaling, Plant Physiol. Am. Soc. Plant Biol. (2006) 330–335, https://doi.org/10.1104/pp.106.078204.

[34] S.S. Gill, N. Tuteja, Reactive oxygen species and antioxidant machinery in abiotic stress tolerance in crop plants, Plant Physiol. Biochem. (December 2010) 909–930, https://doi.org/10.1016/j.plaphy.2010.08.016.

[35] K. Asada, THE WATER-WATER CYCLE IN CHLOROPLASTS: Scavenging of Active Oxygens and Dissipation of Excess Photons, vol. 50, 1999. www.annualreviews.org.

[36] J. Jasper, C. Wagstaff, L. Bell, Growth temperature influences postharvest glucosinolate concentrations and hydrolysis product formation in first and second cuts of rocket salad, Postharvest Biol. Technol. 163 (2020), https://doi.org/10.1016/j.postharvbio.2020.111157.

[37] F. He, B. Thiele, S. Santhiraraja-Abresch, M. Watt, T. Kraska, A. Ulbrich, A.J. Kuhn, Effects of root temperature on the plant growth and food quality of Chinese broccoli (Brassica Oleracea Var. Alboglabra Bailey), Agronomy 10 (5) (2020), https://doi.org/10.3390/agronomy10050702.

[38] R. Kissen, F. Eberl, P. Winge, E. Uleberg, I. Martinussen, A.M. Bones, Effect of growth temperature on glucosinolate profiles in Arabidopsis Thaliana accessions, Phytochemistry 130 (2016) 106–118, https://doi.org/10.1016/j.phytochem.2016.06.003.

[39] V. Ljubej, I. Radojčić Redovniković, B. Salopek-Sondi, A. Smolko, S. Roje, D. Šamec, Chilling and freezing temperature stress differently influence glucosinolates content in Brassica Oleracea Var. Acephala, Plants 10 (7) (2021), https://doi.org/10.3390/plants10071305.

[40] M.S. Almuhayawi, H. AbdElgawad, S.K. Al Jaouni, S. Selim, A.H.A. Hassan, G. Khamis, Elevated CO2 improves glucosinolate metabolism and stimulates anticancer and anti-inflammatory properties of broccoli sprouts, Food Chem. 328 (2020), https://doi.org/10.1016/j.foodchem.2020.127102.

[41] D.N. Karowe, D.H. Seimens, T. Mitchell-Olds, Species-specific response of glucosinolate content to elevated atmospheric Co2 23 (1997).

[42] M.D. López, M.T. Toro, G. Riveros, M. Illanes, F. Noriega, M. Schoebitz, C. García-Viguera, D.A. Moreno, Brassica sprouts exposed to microplastics: effects on phytochemical constituents, Sci. Total Environ. 823 (2022), https://doi.org/10.1016/j.scitotenv.2022.153796.

[43] B. Liese, N.L. Stock, J. Düwel, C. Pilger, T. Huser, C. Müller, Uptake of microplastics and impacts on plant traits of Savoy cabbage, Ecotoxicol. Environ. Saf. 272 (2024), https://doi.org/10.1016/j.ecoenv.2024.116086.

[44] B.A. Halkier, J. Gershenzon, Biology and biochemistry of glucosinolates, Annu. Rev. Plant Biol. (2006) 303–333, https://doi.org/10.1146/annurev.arplant.57.032905.105228.

[45] I.E. Sønderby, F. Geu-Flores, B.A. Halkier, Biosynthesis of glucosinolates - gene discovery and beyond, Trends Plant Sci. (May 2010) 283–290, https://doi.org/10.1016/j.tplants.2010.02.005.

[46] H. Frerigmann, T. Gigolashvili, MYB34, MYB51, and MYB122 distinctly regulate indolic glucosinolate biosynthesis in Arabidopsis Thaliana, Mol. Plant 7 (5) (2014) 814–828, https://doi.org/10.1093/mp/ssu004.

[47] D. Gmižić, M. Pinterić, M. Lazarus, I. Šola, High growing temperature changes nutritional value of broccoli (Brassica Oleracea L. Convar. Botrytis (L.) alef. Var. Cymosa Duch.) seedlings, Foods 12 (3) (2023), https://doi.org/10.3390/foods12030582.

[48] S. Neugart, A. Krumbein, R. Zrenner, Influence of light and temperature on gene expression leading to accumulation of specific flavonol glycosides and hydroxycinnamic acid derivatives in kale (Brassica Oleracea Var. Sabellica), Front. Plant Sci. 7 (MAR2016) (2016), https://doi.org/10.3389/fpls.2016.00326.

[49] S. Neugart, M. Fiol, M. Schreiner, S. Rohn, R. Zrenner, L.W. Kroh, A. Krumbein, Low and moderate photosynthetically active radiation affects the flavonol

glycosides and hydroxycinnamic acid derivatives in kale (Brassica Oleracea Var. Sabellica) dependent on two low temperatures, Plant Physiol. Biochem. 72 (2013) 161–168, https://doi.org/10.1016/j.plaphy.2013.04.002.
[50] A. Lupitu, C. Moisa, S. Gavrilaş, M. Dochia, D. Chambre, V. Ciutină, D. M. Copolovici, L. Copolovici, The influence of elevated CO2 on volatile emissions, photosynthetic characteristics, and pigment content in Brassicaceae plants species and varieties, Plants 11 (7) (2022), https://doi.org/10.3390/plants11070973.
[51] M. Sarfarazi, S.M. Jafari, G. Rajabzadeh, C.M. Galanakis, Evaluation of microwave-assisted extraction technology for separation of bioactive components of saffron (Crocus sativus L.), Ind. Crops Prod. 145 (2020) 111978, https://doi.org/10.1016/j.indcrop.2019.111978.
[52] J. Nagarajan, N.P. Krishnamurthy, R. Nagasundara Ramanan, M.E. Raghunandan, C.M. Galanakis, C.W. Ooi, A facile water-induced complexation of lycopene and pectin from pink guava byproduct: extraction, characterization and kinetic studies, Food Chem. 296 (2019) 47–55, https://doi.org/10.1016/j.foodchem.2019.05.135.
[53] D.A. Herms, W.J. Mattson, THE QUARTERL Y REVIEW OF BIOLOGY THE DILEMMA OF PLANTS: TO GROW OR DEFEND, 1992.
[54] T. Zust, A.A. Agrawal, Trade-offs between plant growth and defense against insect herbivory: an emerging mechanistic synthesis, Annu. Rev. Plant Biol. (2017) 513–534, https://doi.org/10.1146/annurev-arplant-042916.
[55] S. Khaki, L. Wang, Crop yield prediction using deep neural networks, Front. Plant Sci. 10 (2019), https://doi.org/10.3389/fpls.2019.00621.
[56] M. Shahhosseini, G. Hu, I. Huber, S.V. Archontoulis, Coupling machine learning and crop modeling improves crop yield prediction in the US corn belt, Sci. Rep. 11 (1) (2021), https://doi.org/10.1038/s41598-020-80820-1.
[57] G. Leng, J.W. Hall, Predicting spatial and temporal variability in crop yields: an inter-comparison of machine learning, regression and process-based models, Environ. Res. Lett. 15 (4) (2020), https://doi.org/10.1088/1748-9326/ab7b24.
[58] P. Fan, H. Yu, B. Xi, W. Tan, A Review on the Occurrence and Influence of Biodegradable Microplastics in Soil Ecosystems: Are Biodegradable Plastics Substitute or Threat? *Environment International*, vol. 1, Elsevier Ltd May, 2022, https://doi.org/10.1016/j.envint.2022.107244.
[59] T. Song, J. Liu, S. Han, Y. Li, T. Xu, J. Xi, L. Hou, Y. Lin, Effect of conventional and biodegradable microplastics on the soil-soybean system: a perspective on rhizosphere microbial community and soil element cycling, Environ. Int. 190 (2024), https://doi.org/10.1016/j.envint.2024.108781.
[60] L.J. Zantis, S. Adamczyk, S.M. Velmala, B. Adamczyk, M.G. Vijver, W. Peijnenburg, T. Bosker, Comparing the impact of microplastics derived from a biodegradable and a conventional plastic mulch on plant performance, Sci. Total Environ. 935 (2024), https://doi.org/10.1016/j.scitotenv.2024.173265.
[61] Y. Yu, Y. Wang, D.W.S. Tang, S. Xue, M. Liu, V. Geissen, X. Yang, Soil C-N and microbial community were altered by polybutylene adipate terephthalate microplastics, J. Hazard. Mater. 493 (2025), https://doi.org/10.1016/j.jhazmat.2025.138328.
[62] S. Chang, C. Chen, Q.L. Fu, A. Zhou, Z. Hua, F. Zhu, S. Li, H. He, PBAT biodegradable microplastics enhanced organic matter decomposition capacity and CO2 emission in soils with and without straw residue, J. Hazard. Mater. 480 (2024), https://doi.org/10.1016/j.jhazmat.2024.135872.
[63] A. Zhou, Q. Ji, X. Kong, F. Zhu, H. Meng, S. Li, H. He, Response of soil property and microbial community to biodegradable microplastics, conventional microplastics and straw residue, Appl. Soil Ecol. 196 (2024), https://doi.org/10.1016/j.apsoil.2024.105302.